Optics Communications 306 (2013) 121–127

Contents lists available at SciVerse ScienceDirect

Optics Communications

journal homepage: www.elsevier.com/locate/optcom

Interactive holographic three-dimensional display with a spatial mouse

Dongdong Teng, Lilin Liu, Zixin Wang, Yueli Zhang, Biao Wang *,1

School of Physics and Engineering, Sun Yat-Sen University, Guangzhou, Guangdong 510275, PR China

ARTICLE INFO

Article history:
Received 12 February 2013
Received in revised form
3 April 2013
Accepted 13 April 2013
Available online 7 June 2013

Keywords:
CGH
3D display
Interactive
Spatial mouse

ABSTRACT

Based on our previous work (Teng et al., Optics Communication 285, 4235, 2012, [7]), an interactive holographic three-dimensional display system is developed through separating the mirror-image's Fourier CGH of the target object from the planar mirror spatially. A fiber tip is introduced to indicate the spatial content of the displayed light field. Combining with a popup menu, interactive display is realized with the fiber tip as a spatial mouse. The complex amplitude of the zero-order beam caused by the pixelated phase-only spatial light modulator (SLM) is measured through the phase-shifting technology. A hologram which produces not only the functional light patterns but also a corrective beam will be generated to eliminate the zero-order beam through destructive interference. The proposed technology is demonstrated with a 60 Hz SLM by introducing an observer tracking unit.

1. Introduction

Computer generated hologram (CGH) was thought as an ideal three-dimensional (3D) display technique which provides a natural spatial effect. However, limited by the space-bandwidth characteristics of the spatial light modulator (SLM), the viewing angle of the display is very small [1]. Actually, 360° all-around display is the way in which people watch 3D objects in the actual visual space.

A lot of all-around display systems were tried. Otsuka composed a 3D scene with 24 views from different directions horizontally and projected these images onto the rotating directional reflection screen to carry out the 24-view all-around 3D display [2]. Yendo et al. achieved a 360° viewable dynamic color 3D display using the rotating cylindrical parallax barrier and a revolving one-dimensional LED array [3]. Jones set up an all-around display system by projecting over 5000 two-dimensional (2D) images onto a spinning mirror, which was covered by a complicated holographic diffuser to control the diffraction angle of the 2D projection [4]. In some recent reports, Takaki and Uchida replaced the holographic diffuser with a rotating off-axis screen lens. Through a lens shift technique and a image synthesis method, the system was allowed to use multiple projectors, so the number of viewing points increased and the screen rotation speed decreased [5,6]. All the above mentioned systems are based on the binocular parallax technology. The visual accommodation keeps being a problem and the resolution of the light field is limited by the angle-interval between adjacent 2D views.

2. All-around holographic light field display

In our previous work [7], an all-around holographic display system has been proposed to reconstruct the real light field for a viewer moving around. The all-around holographic display system will be reviewed here in brief.

Fig. 1 presents the system schematically. The optical axis is coincident with the z-axis and the SLM is located at the front focal plane of the Fourier transform lens. The codes fed to the SLM generate the Fourier CGH which is denoted as a dashed triangle in the x–z plane in Fig. 1. A planar mirror, with an angle of $\beta = 45^\circ$ to the x–y plane, is used to reflect the CGH. The reflected mirror-image of the CGH, denoted as the solid triangle in the x–z plane, is presented to the viewer. It is a real 3D light field distribution and just the target 3D object to be displayed by the system. The distribution space of the target object is defined as "display zone", which shares the same space with that of the CGH.

Limited by the space-bandwidth characteristics of the SLM, the viewing angle of this displayed target 3D object is very small. To realize all-around 3D display, time-multiplexing technology was used to enlarge the viewing angle. Let the planar mirror keep rotating around the optical axis. Assuming the target 3D object being placed in the "display zone" virtually, at each angular position of the planar mirror, the target 3D object will have one 3D mirror-image with respect to the position, which is denoted as an element mirror-image.

* Corresponding author: Tel.: +86 1343 397 5953.
E-mail address: tengdd@mail.sysu.edu.cn (B. Wang).
1 Current address: School of Physics and Engineering, Sun Yat-Sen University, 135 Xingang West Road, Haizhu District, Guangzhou, Guangdong Province, P.R. China.

0030-4018/$ - see front matter © 2013 Elsevier B.V. All rights reserved.
http://dx.doi.org/10.1016/j.optcom.2013.04.032

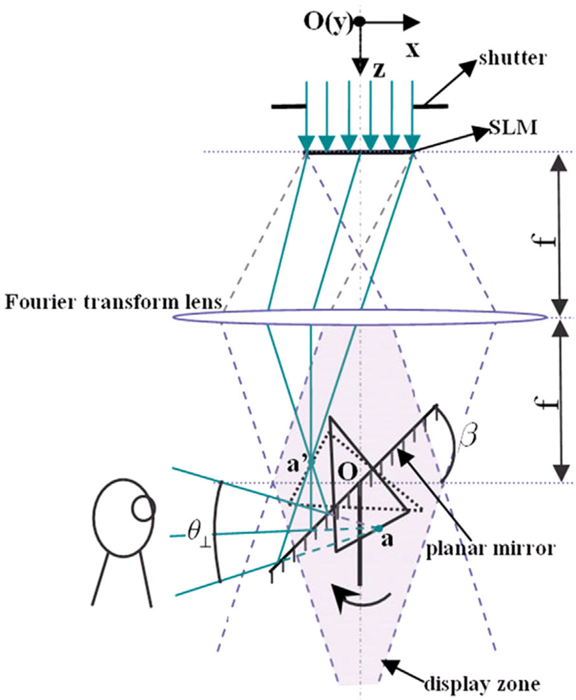

Fig. 1. All-around 3D light field display system.

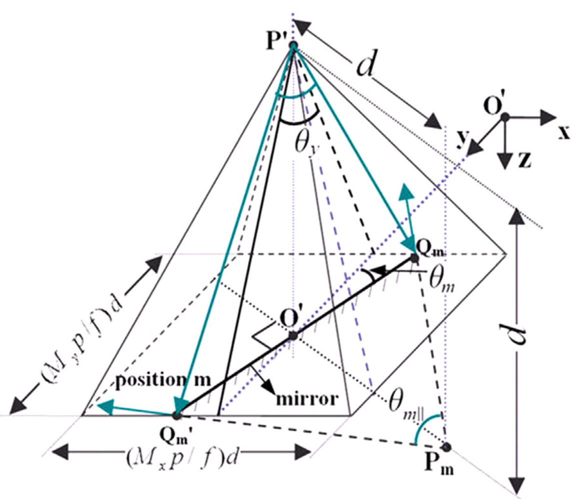

Fig. 2. Geometrical diagram showing the viewing angle distribution with the planar mirror at the position *m*.

When the planar mirror rotates to different angular positions, the corresponding element mirror-image's Fourier CGH is projected onto the mirror by the SLM synchronously. The reflected images reconstruct the target 3D object with different small viewing angle ranges in the *x*–*y* plane. If all these small viewing angle ranges are linked up, all-around holographic light field display can be realized with a SLM of high frame rates per "after image" effects.

Fig. 2 shows the viewing angle distribution of the reconstructed target object in the *x*–*y* plane with the planar mirror rotating to the position *m*. At this position, the planar mirror's angular position is denoted as θ_m, that is, the angle between the negative *y*–axis and the intersecting line of the mirror surface with the *x*–*y* plane. Selecting an arbitrary point P_m on the target 3D object, its viewing angle range is shown in Fig. 2. The mirror point of P_m is on the corresponding CGH and denoted as P'.

Other definitions in Fig. 2 are as follows: *p* denotes the pixel pitch of the SLM, M_x and M_y are the resolutions along the *x* and *y* directions, respectively, *d* is the distance between the point P' and the back focal plane, and the point O' is the projection point. The diffraction zone of P' is proportional to a rectangular pyramid with a bottom face of $(M_x p/f)d \times (M_y p/f)d$ and a height of *d*. The coordinate system has the same definition as that in Fig. 1, except that the coordinate origin is translated to the point O' in Fig. 2.

When the planar mirror rotates to the position *m*, the viewing angle of P_m in the *x*–*y* plane can be expressed as

$$\theta_m = 2\arctan\left(\tan(0.5\,\theta_y)/\cos(\theta_m)\right). \tag{1}$$

where $\theta_y = 2\arctan(M_y p/2f)$ and $\theta_0 = \theta_y$.

According to the geometric relationship shown in Fig. 2,

$$\theta_0/2 + \theta_1/2 = \theta_1 \tag{2}$$

Thus, θ_1 and θ_1 can be obtained. In the same way,

$$\theta_0/2 + \theta_1 + \theta_2/2 = \theta_2 \tag{3}$$

And θ_2 and θ_2 can be obtained. All other angular positions in the 360° range, from θ_3 to θ_N, can be determined by the same method.

3. Interactive holographic three-dimensional display with a spatial mouse

In the present work, the above display system is further developed by introducing in a fibre tip to realized interactive 3D field display. In the following, the interactive 3D field display system is noted as "new" system, while the system reviewed in Section 2 is noted as "old" system.

Compared with those traditional binocular parallax technologies, the main merit of the holographic display lies in that the display point is definitive and its spatial position does not change with the movement of the viewer. Thus, a fiber tip can be introduced into the display field to indicate the display contents as a spatial mouse. The indicated spatial point keeps being the same display point for a moving viewer or viewers at different angular positions around the display system.

The schematic optical diagram of the interactive holographic light field display system with a spatial mouse is shown in Fig. 3.

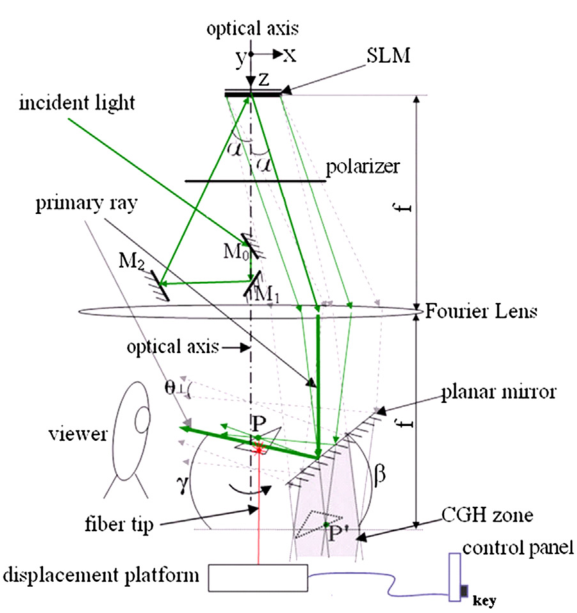

Fig. 3. Schematic optical diagram of the interactive holographic 3D display system.

Compared with Fig. 1, the CGH generated by the SLM is separated from the planar mirror spatially.

Being reflected by the mirror M_0, the incident plane light with circular polarization propagates along the optical axis until arriving at the mirror M_1. The mirror M_1 sends the light beam to the mirror M_2, where the light beam is directed to the SLM with a tilt angle of α. The limited distribution space of the CGH is defined as “CGH zone”. Its 2D distribution in the x–z plane is the shadow region in Fig. 3. The reflected mirror-image of the CGH, denoted as the solid triangle in the x–z plane, is presented to the viewer along the primary ray with a direction angle of γ to the x-y plane. Here the viewing plane is defined as a plane which includes the primary ray and has an angle of γ to the x–y plane. When the values of α and β and the location of the planar mirror are chosen appropriately, the distribution space of the CGH's mirror-image will center around the optical axis and be separated from the planar mirror spatially. This distribution space is the “display zone” of the new interactive display system.

Let mirror M_1, mirror M_2 and the planar mirror keep rotating around the optical axis synchronously. In order to make the SLM's incident beams having the same polarization direction when mirror M_1 and mirror M_2 rotates to different angular positions, a polarizer is placed in front of the SLM to polarize the incident circularly-polarized light. Employing the same time-multiplexing technology as that of the all-around holographic light field display system, the viewing angle range of the light field displayed by the new interactive 3D system can also cover 360° with a SLM of high frame rates. According to the geometric relationship shown in Fig. 3, the variation of β also does not change the object point's viewing angle range in the viewing plane. So, all the angular positions in the new interactive display system are the same as those of the old display system which have been calculated in Section2.

As has been stated, the “display zone” is spatially separated from the planar mirror. A fiber tip on a controllable three-dimensional displacement platform can be introduced into the display zone. The exit light of the fiber is a divergent light spot and can function as a spatial mouse to indicate the spatial content of the displayed light field, as shown in Fig. 3.

The viewer can freely move the mouse through a control panel which is connected to the displacement platform. A left key and a right key are set on the control panel. When the right key is clicked, the feedback system of the displacement platform will record the object point being pointed by the current spatial mouse and a popup menu will be activated in the displayed light field after background processing. The processing begins with obtaining the element mirror-images of the target 3D object with the popup menu by means of image superposing. At each angular position of the planar mirror, a plane containing the same popup menu is inserted into the target object. This plane passes through the center of the display zone and is perpendicular to the primary ray. The mirror-image of the target object with this plane is the element mirror-image of the target object with popup menu at this angular position. To avoid occlusion by the target object, partial contents of the target object that cover the menu along the primary ray are removed. When the planar mirror rotates to different angular positions, the corresponding mirror-image's CGH of the target 3D object with the popup menu is projected by the SLM and the target object with the popup menu is displayed, that is, the popup menu being activated in the displayed light field.

Then, the spatial mouse is moved to an option of the popup menu. The valid region of this option includes the entire scanning space of the option icon when the popup menu rotates around the opitcal axis. When the mouse enters this valid region and the left key is clicked, the feedback system will know that this option is selected. The recorded object point becomes a new datum point. Background image processing programs will be executed basing on the option and a new target object is generated. The new target object will be placed in the display zone virtually and move until the new datum point coincides with the center of the display zone. Using the same technology proposed above, the new object can be displayed.

With all these processes, the interactive all-around 3D holographic display is realized.

4. Elimination of the zero-order beam

Encoding phase-only hologram on a pixelated SLM will project a zero-order beam at the Fourier plane. As an unnecessary illumination, the zero-order beam reduces the functionality of the tailored light pattern. In the present work, to eliminate the zero-order beam, a hologram is designed to produce not only the functional light patterns but also a corrective beam that destructively interferes with the zero-order beam. This is done by applying an additional constraint during the derivation of the phase hologram via a modified iteration algorithms [8]. For the conventional iteration algorithms [9,10], during each loop, the current phase of all the planes keeps invariant, while the current amplitude of a object plane is adjusted to the fixed amplitude distribution of the target Fourier CGH and is adjusted to “1” at the SLM plane. But in the modified iteration algorithms, a complex amplitude which destructively interferes with the zero-order beam is added to the object plane at the back focal plane of the Fourier lens. That is, the current phase is adjusted to the reverse phase of the zero-order beam, the current amplitude distribution is adjusted to the sum amplitude value of the target Fourier CGH and the zero-order beam at the back focal plane during each loop. The amplitude value of the zero-order beam decreases rapidly along the radial direction away from the convergent point. So, only a small region around the convergent point can be considered as the distribution region of the zero-order beam, which is defined as the “valid region”. At the back focal plane, the current phase needs to be adjusted only in this small “valid region” and keeps invariant outside this small region. As a result, the convergence of the modified iteration algorithms does not deteriorate due to the introduction of the additional constraint.

The complex-amplitude value of the zero-order beam, $U_{zero}(x,y)=A_{zero}\exp(i\varphi_{zero})$, is measured by the phase-shifting technology [11] in the present article. A plane pattern with a black circular region centered around the “valid region” is generated by the SLM at the back focal plane. The zero-order beam will generate a light spot at the center of the black circular region. An aperture is placed just at the location of the plane to block the generated pattern except for the black circular region. A reference light, $U_{ref}(x,y)=A_{ref}\exp(i\varphi_{ref})$, is directed to interfere with the zero-order beam. The amplitudes of the zero-order beam or the reference beam can be detected respectively by a CCD camera at the back focal plane with the the other beam being blocked. The phase of the reference waves is changed in a stepwise manner, and each resulted interference fringe is detected. The intensity of the resulted interference fringe being recorded by the CCD camera is expressed as:

$$I(x,y,\varphi_{ref})=\left|U_{zero}(x,y)+U_{ref}(x,y)\right|^2=A_{zero}^2+A_{ref}^2 \\ +2A_{zero}A_{ref}\cos(\varphi_{ref}-\varphi_{zero}) \tag{4}$$

where A_{ref}, A_{zero}, φ_{ref}, φ_{zero} denote the amplitudes and phases of the reference light and the zero-order beam light, respectively.

Substituting the detected intensity values of the above interference fringes with incremental phase by a step of $\pi/2$ from 0 to

2π, the phase of the zero-order beam is derived as

$$\varphi_{zero}(x,y) = \tan^{-1}[(I(x,y,3\pi/2) - I(x,y,\pi/2))/(I(x,y,0) - I(x,y,\pi))] \quad (5)$$

where the initial reference phase has been assumed to zero.

At different angular positions, the inclination angle of the incident plane light with respect to the z-axis, α is not changed in value, while those with respect to the x-axis and y-axis keep changing, as shown in Fig. 3. At the angular position m, with θ_{xm} and θ_{ym} denoting the inclination angles with respect to the x-axis and y-axis, the light field of the zero-order beam at the back focal plane can be expressed as:

$$\begin{aligned} U_{zero\ m}(x,y) &= \mathbb{F}\left(f(x_0,y_0)\exp(jkz\cos\ \alpha)\exp(jk(x_0\cos\theta_{xm} + y_0\cos\theta_{ym}))\right) \\ &= \exp(jkz\cos\ \alpha)\mathbb{F}\left(f(x_0,y_0)\exp(j2\pi(x_0\cos\theta_{xm}/\lambda + y_0\cos\theta_{ym}/\lambda))\right) \\ &= cons^{*}U(x - f\cos\theta_{xm}, y - f\cos\theta_{ym}) \end{aligned} \quad (6)$$

where $f(x_0, y_0)$ denotes the complex amplitude distribution at the SLM plane which results in the zero-order beam, and $U(x,y)$ is the Fourier transformation of $f(x_0,y_0)$ through the Fourier transform lens, f and "cons" represent the Fourier transform Operator and a constant value, respectively. Eq. (6) proves that the phase and amplitude distributions of the zero-order beams remain unchanged when the mirror M_1 and mirror M_2 rotate to different angular positions, although a relative 2-D translation at the plane perpendicular with the optical axis occurs. So, in our experimental system, only a single measurement is needed.

5. Experiment and results

A display system is set up to implement the idea described above, as shown in Fig. 4. One HEO-1080 SLM from Holoeye Photonics AG with the frame rate of 60 Hz is used for computer-generated hologram coding. The SLM is a pure phase modulator with a resolution of 1920×1080 and pixel size of $8 \times 8\ \mu m^2$. The incident linearly polarized beam is provided by a laser with a wavelength of 532 nm. It is converted into a circularly polarized light through a 1/4 wave plate. The circularly polarized light is directed to the SLM through reflections of four planar mirrors: M_3, M_0, M_1 and M_2. Another polarizer is placed in front of the SLM to ensure the same polarization direction of SLM's incident beams when mirror M_1 and mirror M_2 rotate to different angular positions. A mechanical frame with a display window is fixed on the rotating platform. Mirror M_1, M_2 and the Fourier lens are attached to the mechanical frame and rotate with the rotating platform synchronously. The Fourier lens has a focal length of 150 mm. The inclination angles are set as $\alpha = 6°$ and $\beta = 35°$. So $\gamma = 20°$, which means that the viewer overlooks the displayed object by an angle of 20°. According to the calculation method shown above, $N = 84$ different element mirror-images are needed.

In order to measure the complex amplitude value of the zero-order beam, a two-beam interferometer is set up, as shown in Fig. 5. The SLM, Fourier lens and incident angle of α are the same as those in Fig. 4 so as to make sure the zero-oder beam being identical.

A square white region with a central black circular region, as shown in Fig. 6(a), is set as the target Fourier transform CGH for the phase-shifting system described in Fig. 5. It should be noted that the diameter of the black circular is one third of the side length of the square. Zones 1 and 2 refer to the circumscribed square and the inscribed square of the black circular, respectively. Conventional iteration algorithms are used for holographic encoding to generate this square pattern at the back focal plane. In this procedure, 200 loops were executed. A circular aperture which is a little smaller than the black circular region was adopted to block the generated hologram. The captured image in the zone 1 is shown in Fig.6(b). The zero-order beam can been seen and its strength distribution in zone 2 is shown in Fig.6(c). According to the the strength distribution, the "valid region" is set to be a central square region with a side length of two fifth of the zone 1's

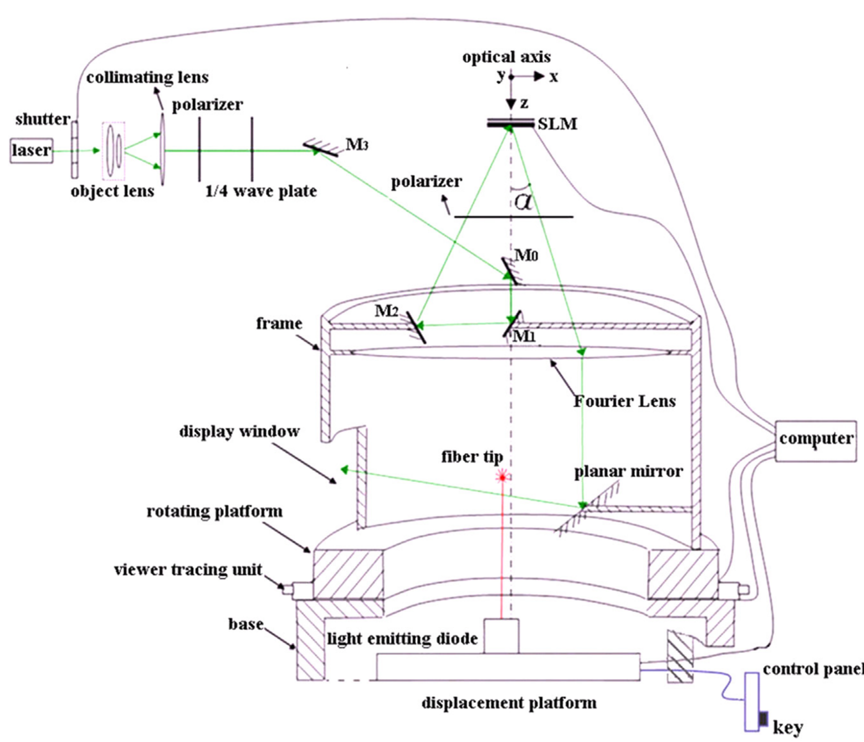

Fig. 4. Schematic drawing of the experimental setup.

side length. Outside the "valid region", the detected strength is weak and nearly constant, which can be seen as the system noise which is independent of the zero-order beam.

In order to obtain the phase distribution in the "valid region", a reference light was introduced to interfere with the zero-order beam as indicated in Fig. 5 with $\theta = 4°$. Four interference fringes are obtained through different phase shifting plates, which are inserted into the reference light to retard its phase by 0, $\pi/2$, π and $3\pi/2$, respectively. The interference fringes are recorded with CCD. Thus, the phase distribution of the zero-order beam can be derived according to Eq.(5), as shown in Fig. 6(d).

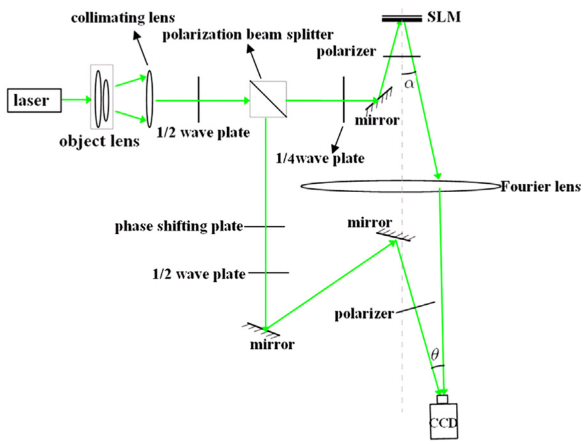

Fig. 5. Schematic diagram showing the phase-shifting technology.

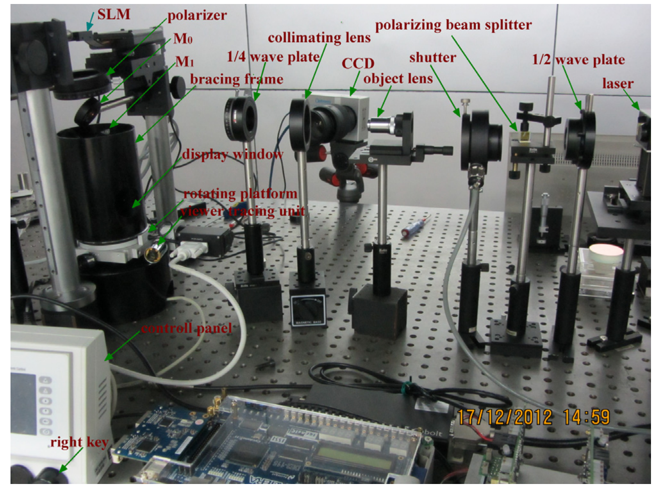

Fig. 7. Photograph of the experimental display system.

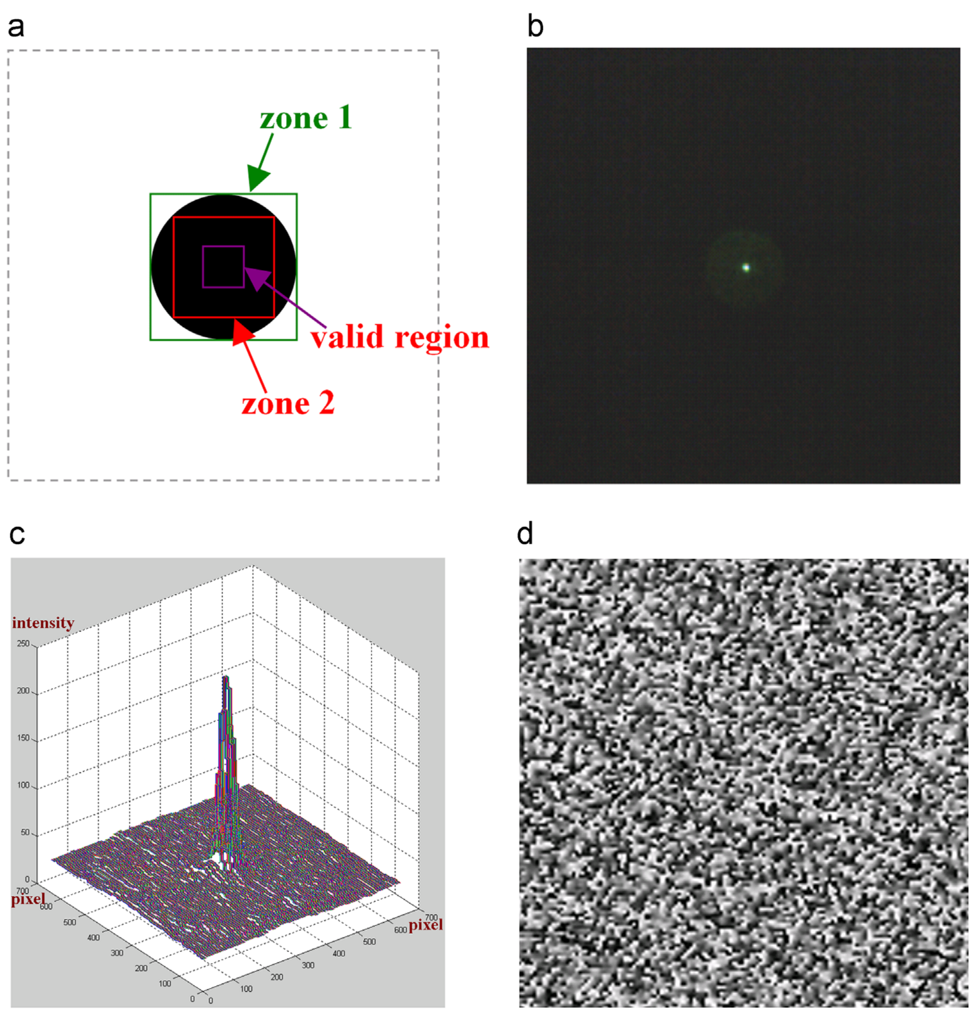

Fig. 6. (a) Target pattern for the phase-shifting technology, (b) captured image in zone 1, (c) detected strength distribution in zone 2 and (d) derived phase distribution in "valid region".

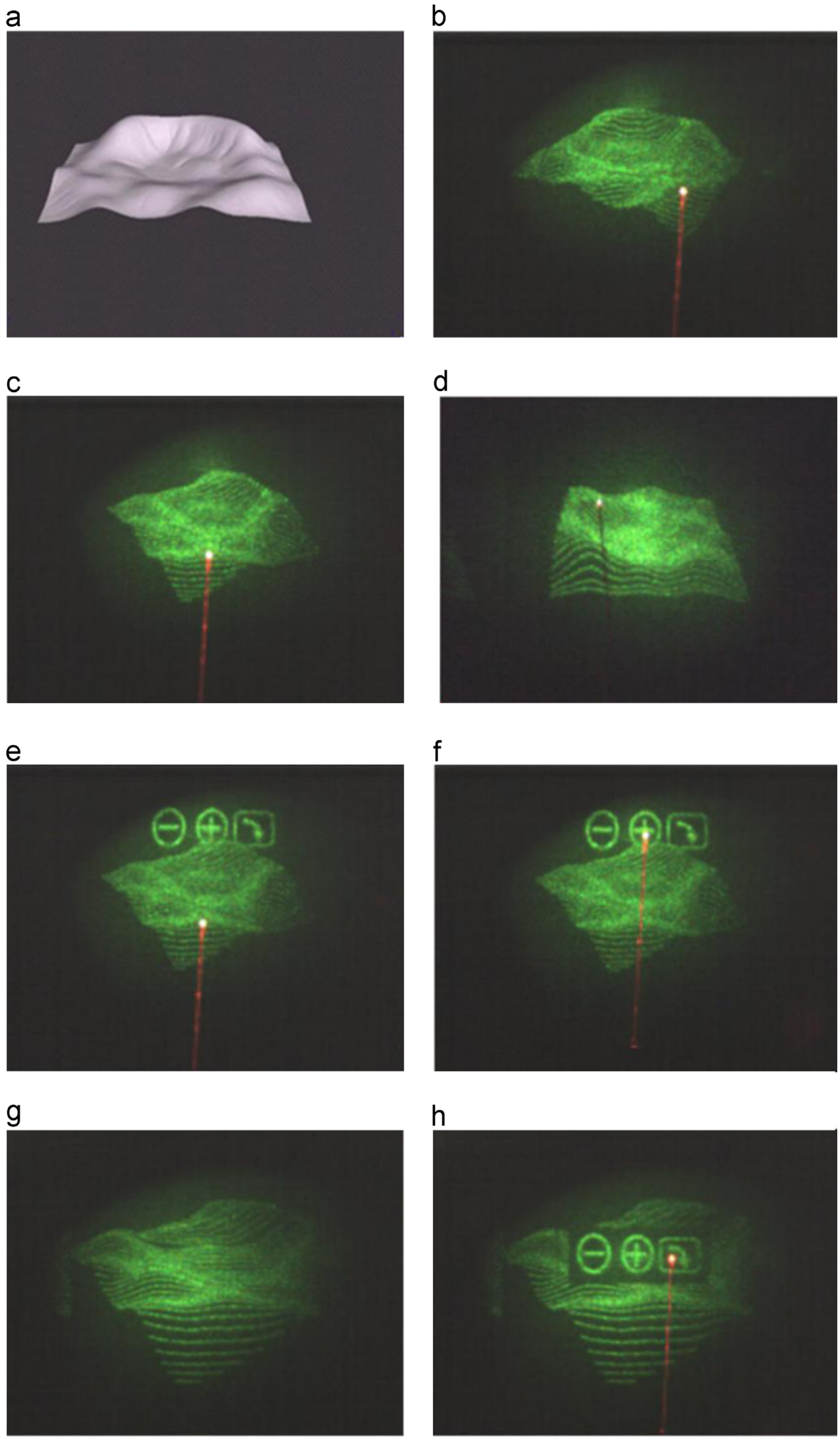

Fig. 8. Captured images when the display system works: (a) the original terrain, (b) spatial mouse points to a chosen object point of the 3D terrain with the camera being at the position 1, (c) spatial mouse points to the same chosen object point of the 3D terrain with the camera being at the position 2, (d) spatial mouse points to the same chosen object point of the 3D terrain with the camera being at the position 3, (e) 3D terrain with the popup menu when the camera being at the position 2, (f) spatial mouse points to the "zooming out" option on the popup menu, (g) enlarged view of the 3D terrain with the spatial mouse being shut off, and (h) clicking the "restoration" option on the popup menu.

Using above phase and amplitude distributions of the zero-order beam in the "valid region", phase codes of the element mirror-images are obtained with the proposed modified iteration algorithms. In the present experiment, 200 loops were executed and an element mirror-image was divided into 52 object planes.

Because the frame rate of the SLM used in the experiment is not high enough, obvious image flicker is unavoided. A viewer tracing unit is introduced in to solve this problem by detecting the position of the viewer. Only CGHs of the chosen three neighboured element mirror-images are projected. The fused visual range of these three CGH's mirror images is about 10°, which is wide enough to cover the two eyes of the viewer who is 300 mm away from the display system.

The rotating platform keeps rotating at the speed of 60 rps. In each rotating cycle of the rotating platform in Fig. 4, phase codes of a chosen element mirror-image are fed to the SLM and the shutter in the light path closes until the planar mirror rotates to the corresponding angular position. An acoustooptic deflector supported by a bracing frame is taken as the shutter, which is placed before the beam expanding object lens. When the acoustooptic deflector works, the incident laser beam will be deflected from the input aperture of the object lens, thus the incident light of the SLM is closed. The adopted acoustooptic diflector is 46080-1-LTD from Gooch & Housego. The rise time is 150 ns/mm and the acoustic aperture size is 1 mm.

Three chosen element mirror-images are projected onto the rotating planar mirror alternately and cyclically in time sequence. The chosen three neighboured element mirror-images change with the position of the moving viewer. Hence, by introducing in such a viewer tracing unit, all-around holographic 3D display can be realized with a SLM of 60 Hz. The refresh rate of the display system reaches 20 Hz and no obvious image flicker is observed. Fig. 7 is the photograph of the experimental display system.

A 3D terrain of $9.0 \times 9.0 \times 6.75\text{mm}^3$ is displayed to demonstrate the developed technology and system. Since the displayed points will rotate around the optical axis along with the rotating planar mirror, image blur occurs in our proposed display system. In order to solve this problem, the opening time of the shutter is set as small as 20 μs. Therefore the displayed points scanning size during the opening time will be not more than 34 μm. In our experiment, the resolution of the projected CGH is set to be 400×400. Then, the corresponding distance between two adjacent displayed points is about 25 μm, which is close to 34 μm. So, no obvious image blur is observed in the experiment.

Fig.7(a) shows the original terrain. The red incident beam in the fibre is coupled from a light emitting diode. Using a camera to replace the viewer, images when the camera moves to the angular position 1, 2 and 3 around the display system are captured, as shown in Fig.8(b–d). The angular interval between position 1 and position 2 is 30°, and that between position 2 and position 3 is 210°. When the camera moves to and stays at position 2, clicking the right key on the control panel, the system will load CGH codes of element mirror-images containing the popup menu. The captured image changes to Fig.8(e). The popup menu includes three option icons: 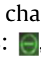, and , representing "zooming in", "zooming out" and "restoration", respectively. As an example, moving the mouse to the "zooming out" option and clicking the left key, as shown in Fig. 8(f), the enlarged image is displayed. The corresponding enlarged images are shown in Fig. 8(g) and (h). If shutting down the light in the fiber, the captured image demonstrates that the introduction of such a mouse has no effect on the displayed light field, see Fig. 8(g). If the "restoration" option is clicked, as shown in Fig. 8(h), the system will go back to display the original target object, as shown in Fig. 8(c).

6. Couclusion

A novel interactive holographic 3D display with a fiber tip as the spatial mouse is proposed and implemented in the present work. The key idea lies in separating the displayed target light field from the rotating planar mirror of the all-around holographic 3D display system spatially. Thus a fiber tip can be introduced into the displayed target light field to indicate the spatial content. As a spatial mouse, it can active the popup menu in the displayed 3D light field and manipulate the displayed content according to the selected menu item. In addition, the zero-order beam, as an unnecessary illumination caused by the pixelated phase-only SLM, is eliminated through a generated hologram which produces not only the functional light patterns but also a corrective beam. The corrective beam will interference with the zero-order beam destructively. The phase-shifting technology is employed to measure the complex amplitude of the zero-order beam. Experimentally, the interactive holographic 3D display is demonstrated with a 60 Hz SLM by introducing an observer tracking unit. Limited by performances of the SLM used in the present work, the display system only accommodates one observer. Using a SLM with higher frame rates, a multi-observer interactive display system can be implemented by the proposed technology. As a matter of fact, some ferroelectric SLMs with frame rates of thousands Hz begin to appear on the market [12].

Acknowledgement

This paper was supported by the Natural Science Foundation of China under Grant no. 10802101, Reserve fund Natural Science Foundation of China under Grant nos. (61172027, 11072271, 10972239, and 61007026) and Personnel Training of Sun Yat-Sen University under Grant no. 1132493.

References

[1] J.W. Goodman, Introduction to Fourier Optics, McGraw-Hill, 1996, p. 352-353.
[2] R. Otsuka, Transport: all-around display system for 3D solid image, IEEE Transactions on Visualization and Computer Graphics 12 (2006) 178–185.
[3] T. Yendo, T. Fujii, M. Tanimoto, M.P. Tehrani, The seelinder:cylindrical 3D display viewable from 360°, Journal of Visual Communication and Image Representation 21 (5–6) (2010) 586–594.
[4] A. Jones, I. McDowall, H. Yamada, M. Bolas, P. Debevec, Rendering for an interactive 360° light field display, ACM Transactions on Graphics 26 (3) (2007) 40.
[5] S. Uchida, Y. Takaki, 360-Degree three-dimensional table-screen display using small array of high-speed projectors, Proceedings of the SPIE 8288 (2012) 82880D.
[6] Y. Takaki, S. Uchida, Table screen 360-degree three-dimensional display using a small array of high-speed projectors, Optics Express 20 (5) (2012) 8848–8861.
[7] D.D. Teng, L.L. Liu, Z.X. Wang, B. Wang, All-around holographic three-dimensional light field display, Optics Communications 285 (21–22) (2012) 4235–4240.
[8] D. Palima, V.R Daria, Holographic projection of arbitrary light patterns with a suppressed zero-order beam, Applied Optics 46 (20) (2007) 4197.
[9] M. Makowski, G. Mikula, M. Sypek, A. Kolodziejczyk, Three-plane phase-only computer hologram generated with iterative Fresnel algorithm, Optical Engineering 44 (2005) 125805.
[10] M. Makowski, M. Sypek, A. Kolodziejczyk, G. Mikula, J. Suszek, Iterative design of multiplane holograms:experiments and applications, Optical Engineering 46 (2007) 045802.
[11] I. Yamaguchi, T. Zhang, Phase-shifting digital holography, Optics Letters 22 (16) (1997) 1268–1270.
[12] ⟨http://www.bnonlinear.com/products/xyslm/flc.pdf⟩.